

All Optical Three Dimensional Spatio-Temporal Correlator for Automatic Event Recognition Using Multiphoton Atomic System

Mehjabin S. Monjur,^{1,*} Mohamed F. Fouda,¹ and Selim M. Shahriar^{1,2}

¹*Department of Electrical Engineering and Computer Science, Northwestern University,
Evanston, IL 60208, USA*

²*Department of Physics and Astronomy, Northwestern University, Evanston, IL 60208, USA*

**Corresponding author: mehjabin@northwestern.edu*

In this paper, we model and show the simulation results of a three-dimensional spatio-temporal correlator (STC) that combines the technique of holographic correlation and photon echo based temporal pattern recognition. The STC is shift invariant in space and time. It can be used to recognize rapidly an event (e.g., a short video clip) that may be present in a large video file, and determine the temporal location of the event. It can also determine multiple matches automatically if the event occurs more than once. We show how to realize the STC using Raman transitions in Rb atomic vapor.

OCIS codes: (070.0070) Fourier optics and signal processing; (070.4550) Correlators.

1. Introduction

Automated target recognition (ATR) has been a very active field of research for several decades. Significant advances in ATR have been made using analog approaches employing holographic correlators, as well as computational approaches using dedicated digital signal processing (DSP) chips or softwares. However, these techniques are inadequate for the task of automatic event recognition (AER). AER is defined as the task of identifying the occurrence of an event within a large video data base. The goal of an AER system is to determine if these events occurred, when they occurred, and how many times. In principle, this can be achieved by searching through each frame in the data base, and comparing them with reference images. This process is prohibitively time consuming, even with a very efficient optical image correlator, a software or a DSP based image recognition system. However, by employing the properties of atoms [1,2,3,4,5] it is possible to realize an AER that can recognize rapidly the occurrence of events, the number of events, and the occurrence times. In this paper, we describe quantitatively the design and show the simulation results of an AER system in the form of a three-dimensional spatio-temporal

correlator (STC) that combines the technique of holographic correlation and the technique of photon echo based temporal pattern recognition.

Shift invariant in space and time, the STC can recognize rapidly an event that may be present in a video file, and determine the temporal location of the event. In general, modeling the STC requires determining the temporal dynamics of a large number inhomogeneously broadened atoms, multiplexed with free-space wave propagation equations. Here, along with modeling the STC using the Schrodinger equation for the temporal evolution of atoms excited by optical fields, we show that the response of the STC can be determined by modeling the response of the interaction medium as a simple, three-dimensional, multiplicative transfer function in the spatio-temporal Fourier domain. We explain the physical origin of this model, and then establish the validity of this model by comparing its prediction with that determined via the quantum mechanical dynamics. We then show some examples of the response of the STC using both methods.

2. Translation Invariant Spatial Holographic Correlator (TI-SHC)

The simplest version of the Translation Invariant Spatial Holographic Correlator (TI-SHC) is illustrated schematically in figure 1. In figure 1(a), we show the initial step, where a reference image (denoted as $U_{A1}(x_1, y_1)$) at the plane P_1 , is first passed through a lens of focal length L , which produces a two-dimensional, spatial Fourier Transform (FT) of the image in the plane of the holographic medium P_M . The FT the reference image, $U_{A1}(x_1, y_1)$ can be written as:

$$U_{AM}(x_M, y_M) = \frac{e^{j2kL}}{j\lambda L} \cdot \tilde{U}_{A1}\left(\frac{kx_M}{L}, \frac{ky_M}{L}\right) \quad (1)$$

where \tilde{U}_{A1} is the Fourier Transform of U_{A1} . A plane writing wave is applied at an angle ϕ in the y-z plane, to interfere with the transformed image in the plane, P_M . This writing plane wave can be written as:

$$U_W(x_M, y_M) = U_{W0} e^{-jk_\phi y_M}; \quad k_\phi = k \sin \phi \quad (2)$$

where k is the wave number of the laser field. The interference between the plane and the FT of the reference image is recorded in a thin photographic plate, which produces a transmission function that is proportional to the interference pattern:

$$t(x_M, y_M) = \alpha I(x_M, y_M); (x_M, y_M) = |U_{AM}(x_M, y_M) + U_W(x_M, y_M)|^2 \quad (3)$$

For simplicity, we will assume that $\alpha = 1$, so that:

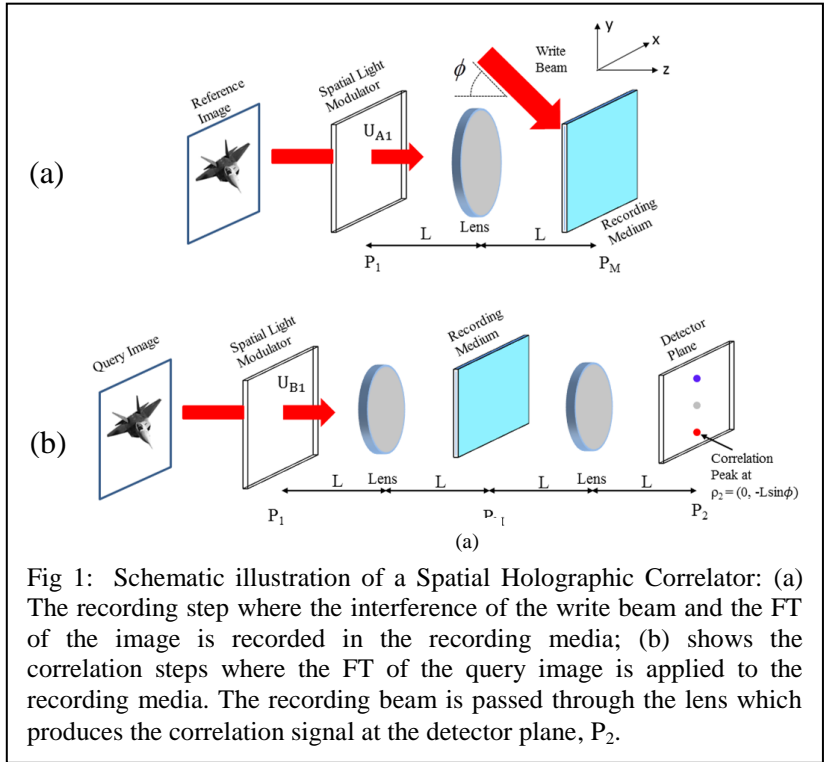
$$t(x_M, y_M) = t_1 + t_2 + t_3 + t_4 \quad (4)$$

$$t_1 = U_{W0}^2; \quad t_2 = |U_{AM}|^2; \quad t_3 = U_{W0}U_{AM}^*e^{-jk_\phi y_M}; \quad t_4 = t_3^* = U_{W0}U_{AM}e^{jk_\phi y_M}$$

Next, a query image, $U_{B1}(x_1, y_1)$ is passed through the same lens, thus producing its FT $U_{BM,b}(x_M, y_M)$, which is then applied to the holographic medium, as shown in figure 1(b). After passing through the photographic plate, the field can be written as:

$$U_{BM,a}(x_M, y_M) = tU_{BM,b}(x_M, y_M) = (t_1 + t_2 + t_3 + t_4)U_{BM,b}(x_M, y_M) \quad (5)$$

Only the term proportional to t_3 produces the cross-correlation signal. The transmitted beam is then passed through another lens. In the FT plane of this lens, a signal corresponding to the cross-correlation between the reference image and the query image is observed. The signal is the strongest if the query image is identical to the reference image, and appears at a location determined by the angle ϕ of the writing beam. If the query image is the same as the reference image, but translated laterally, the peak remains equally strong, and is shifted by an amount that corresponds to this translation



[6,7,8,9]. In general the correlation signal can be written as:

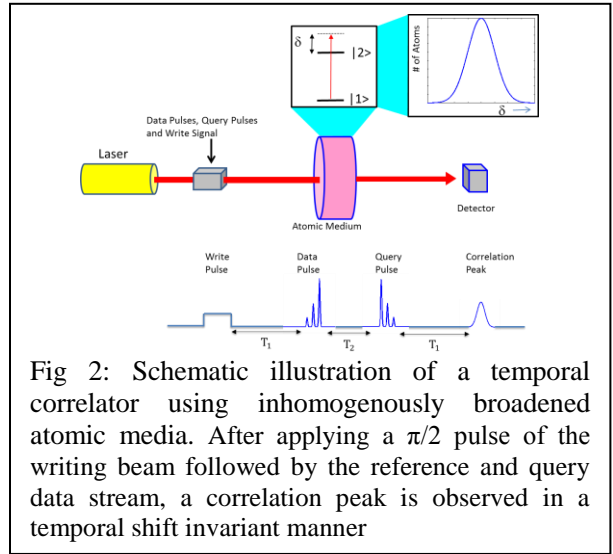
$$S_{CC}(\rho_2) = IFFT\{U_{W0}U_{AM}^*e^{-jk_\phi y_M}U_{BM,b}\} \quad (6)$$

It is also possible to realize the TI-SHC as a single-step process, where the write beam, the reference beam and the query beams are applied simultaneously to a dynamic photo-refractive medium, thus realizing what is known as the joint-transform correlator [10]. Using

images pre-processed via so-called polar Mellin transforms, it is also possible to make the system invariant with respect to scale and rotation.

3. Translation Invariant Temporal Correlator (TI-TC)

To illustrate the Translation Invariant Temporal Correlator (TI-TC), consider a medium that is inhomogeneously broadened, meaning that the atoms inside the medium have a range of resonant frequencies. In such a medium, one can record a temporal data sequence by using a uniform recording pulse separated in time. The mathematical modeling of such a system is discussed in appendix A. The medium stores the FT of the combined temporal signal. A matching but temporally



reversed data stream applied later on produces a single pulse, indicating data correlation [11,12, 13,14,15,16,17]. This is illustrated schematically in figure 2, which shows the simulation results of a temporal correlation in an inhomogeneously broadened atomic medium. Figure 2 is simulated using the quantum mechanical amplitude equations described in Appendix A. This is achieved by applying a $\pi/2$ pulse of the writing beam, followed by the query data stream, with a certain time lag. When the reference data stream is applied to this memory, a correlation peak is observed in a temporally shift invariant manner. In the simulation shown here, we have used an idealized, decay-free two level system of atoms with an inhomogeneous broadening that is larger than the inverse of the temporal resolution of the data stream. In appendix B, we have shown that, an off-resonant excitation in a three-level system can be shown to be equivalent to this model. The photon echo process can be modeled by the following equation:

$$\tilde{D}(f_T) = \tilde{A}(f_T)^* * \tilde{B}(f_T) * \tilde{C}(f_T) \quad (7)$$

$$S_{out} = \text{IFFT}(\tilde{D}(f_T)) = S(t - T_2 - T_3 + T_1) \quad (8)$$

where $\tilde{A}(f_T) = \text{FT of the reference } \pi/2 \text{ pulse}$; $\tilde{B}(f_T) = \text{FT of the query pulse}$; $\tilde{C}(f_T) = \text{FT reference pulse train}$.

There is a close analogy between this process and the holographic spatial correlator. The initial data stream corresponds to the reference image, and the recording pulse corresponds to the write beam, with the time separation being analogous to the angle between the reference image and the write beam. The matching pulse corresponds to the query image, and the output pulse corresponds to the correlation. Just as in the case of spatial holography, the process is translation invariant, meaning that if the matching pulse is shifted in time, the correlation peak appears at a different time, but with the same strength. This is again due to the fact that the FTs of two data streams that are identical but shifted in time have the same intensities, and differ only in phase. Finally, it should be noted that using Mellin transform [18] in the time domain, it is possible to make this correlator function in a scale invariant manner.

4. Automatic Event Recognition (AER) via Translation-Invariant Spatio-Temporal Correlator

The natural extension to searching for images in spatial domain and searching for signals in time is to search for an image that is changing in time, which is simply a video clip corresponding to an event. Consider a video signal, either from a live camera feed or from a DVD player, for example. The video signal is an image that is changing in time, i.e. it has both spatial and temporal properties. An AER system can recognize a short clip within that video feed, by using Translation Invariant Spatio-Temporal Correlator (TI-STC) which is a combination of the TI-SHC and the TI-TC.

The AER process is illustrated schematically in figure 3. In figure 3(a), we

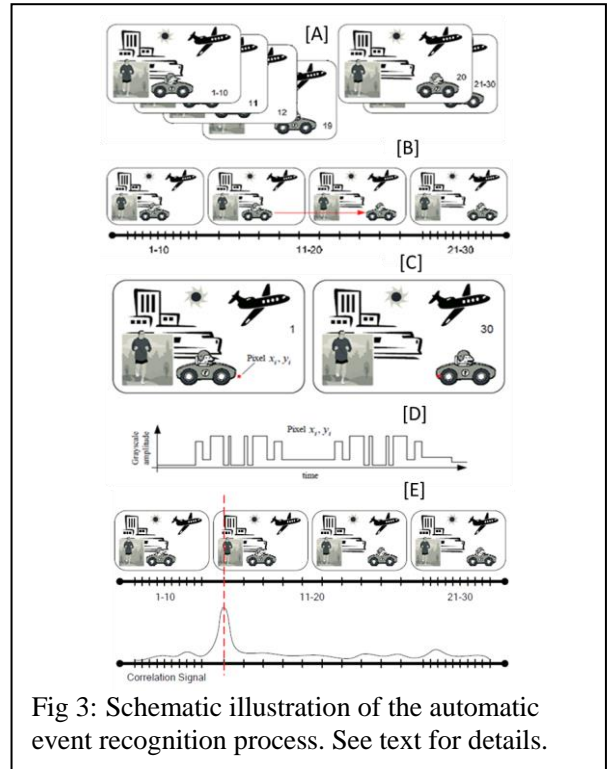
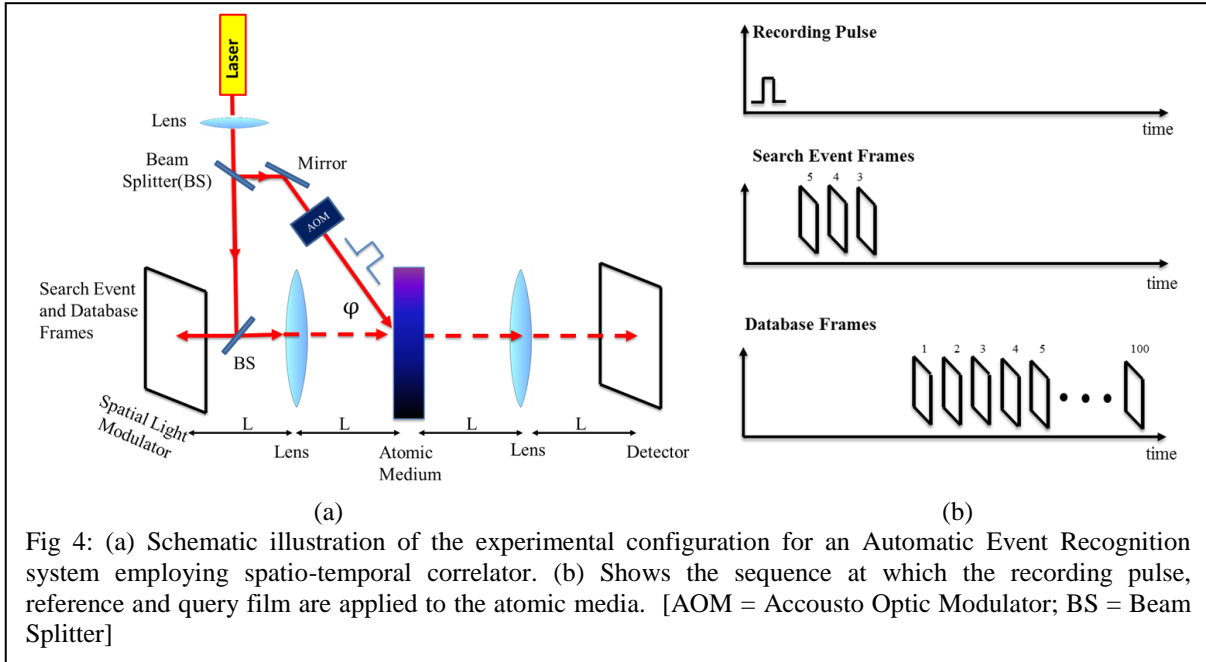


Fig 3: Schematic illustration of the automatic event recognition process. See text for details.

show a series of 30 consecutive frames in a video. Frames 1-10 are of a static, unchanging scene. In frame 11 a car begins to drive across the scene, and stops in frame 20. Frames 21-30 are again static. This is illustrated in figure 3(b). If we consider a single pixel from this video signal, as indicated in figure 3(c), the resulting pattern as the car moves from one place in frame 11 to another in frame 20 is shown in figure 3(d). This signal is akin to the signals we used in the temporal signal correlation example in section 3. Each pixel in the video will have a corresponding bit stream, which could all be recognized separately in a temporal correlator. However, by combining the spatial correlator, we can now recognize a group of pixels that form an image, as they change in time.

As an example, consider the case where the event to be recognized is the car driving from one place to another. In the AER system, the whole video will be the database, and the ten clips corresponding to the movement of the car will be the query event. The output correlation signal in the AER system will contain a correlation peak at the time corresponding to frame 11, where the start of the query event occurs, as illustrated in figure 3(e). Because the system is translation invariant spatially, we can find the car driving across the scene no matter where it occurs within the frame. Furthermore, because the system is translation invariant in time as well, no a priori knowledge regarding the start time of the query event within the database video is necessary. Furthermore, the time at which the correlation peak will appear can be used to infer the location of the query event within the database video. It should also be noted that if the same event occurs N times within the database video, N different correlation peaks will be observed. Finally, if the polar Mellin transform [18] is used to pre-process each of the frames in the database video as well as the query video, it would be possible to recognize the event even when the images in the query clip are scaled and rotated with respect to the databased video.

5. Architecture of the Spatio-Temporal Correlator (STC)



The experimental configuration for realizing the AER system is illustrated schematically in figure 4. The architecture for the AER system is similar to that of a conventional spatial holographic correlator except that the write pulse is replaced by a plane wave of certain duration and the recording medium is replaced by the inhomogeneously broadened atomic medium (AM). The laser beam is split into two ports using a beam splitter (BS); one of the ports is fed to the acousto-optic modulator (AOM) which creates the recording pulse. Another beam is used to retrieve the query frames and database video frames from the spatial light modulator (SLM). At time T_1 , the recording pulse is applied to the AM. At time T_2 , the query frames, which are retrieved from the SLM, pass through the lens and are then applied to the AM. The lens produces a two dimensional Fourier Transform (2D-FT) of each frame. Thus, the interference of the recording pulse and the 2D-FTs of the query frames are stored in the AM. At time T_3 , the database video frames are retrieved from the SLM and the 2D-FT of those frames are applied to the AM. Then the signal from the AM passes through another lens and the detector array records the output signals as functions of time. The output signal, integrated spatially over the detector array, contains a correlation peak at a time corresponding to the position where the matching pattern occurs in the database video. This is, of course, the desired functionality of the AER.

The behavior of the system can be simulated explicitly using quantum mechanical evolution dynamics of atoms excited by laser fields [12,19]. However, the response of the atomic system can also be modeled using a single transfer function:

$$\tilde{D}(f_T, k_x, k_y) = \tilde{A}(f_T, k_x, k_y)^* \tilde{B}(f_T, k_x, k_y) \tilde{C}(f_T, k_x, k_y) \quad (9)$$

$$S_{out} = \text{IFFT}(\tilde{D}(f_T, k_x, k_y)) = S(t - T_2 - T_3 + T_1, x, y) \quad (10)$$

where, $\tilde{A}(f_T, k_x, k_y)$ = FT of the reference pulse; $\tilde{B}(f_T, k_x, k_y)$ = FT of the query video frames; $\tilde{C}(f_T, k_x, k_y)$ = FT database reference video frames. Note that, in the FT domain, the output is the product of three functions: the conjugate of the FT of the recording pulse, the FT of the query frames, and the FT of the database frames. Note also that these are FTs in three dimensions: the two spatial dimensions and the time dimension. The FT in the two spatial dimensions is realized by the lens, and the FT in time is accomplished by the atomic media. Thus, in the physical domain, the output is a three-dimensional cross-correlation between the query frames and the database frames, shifted in space and time.

6. Simulation Results

For a given pixel, the upper graph of Fig 5 shows the simulation results of a temporal correlator in an inhomogeneously broadened atomic medium. The details of the modeling of the system have been discussed in appendix A. To simulate the temporal correlator using the atomic system, we have to apply a $\pi/2$ pulse of the

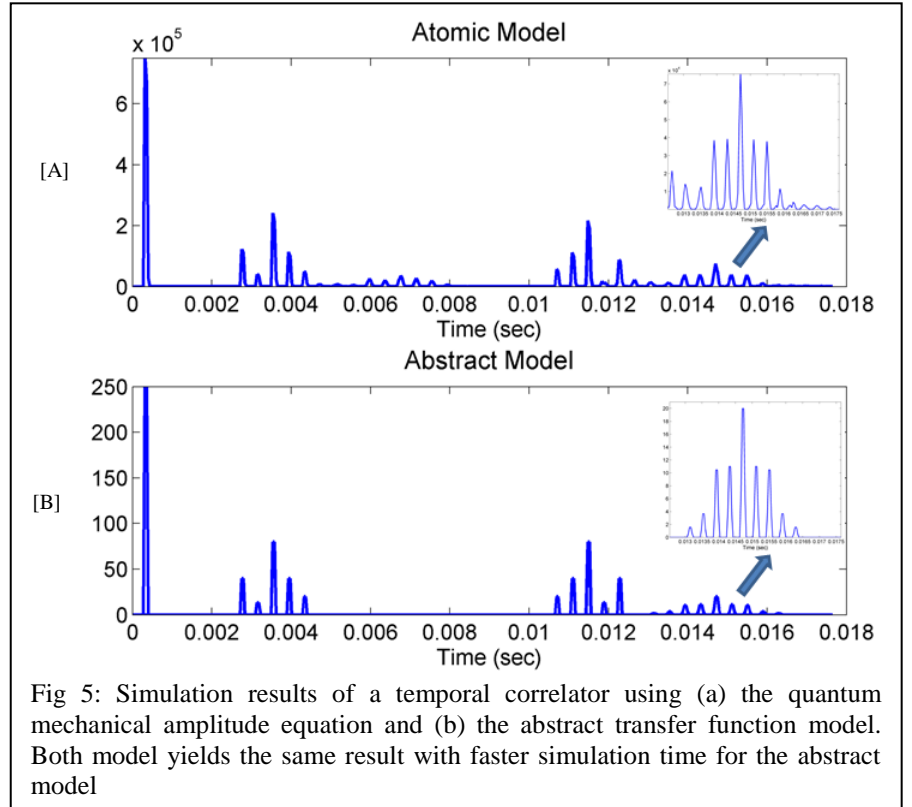
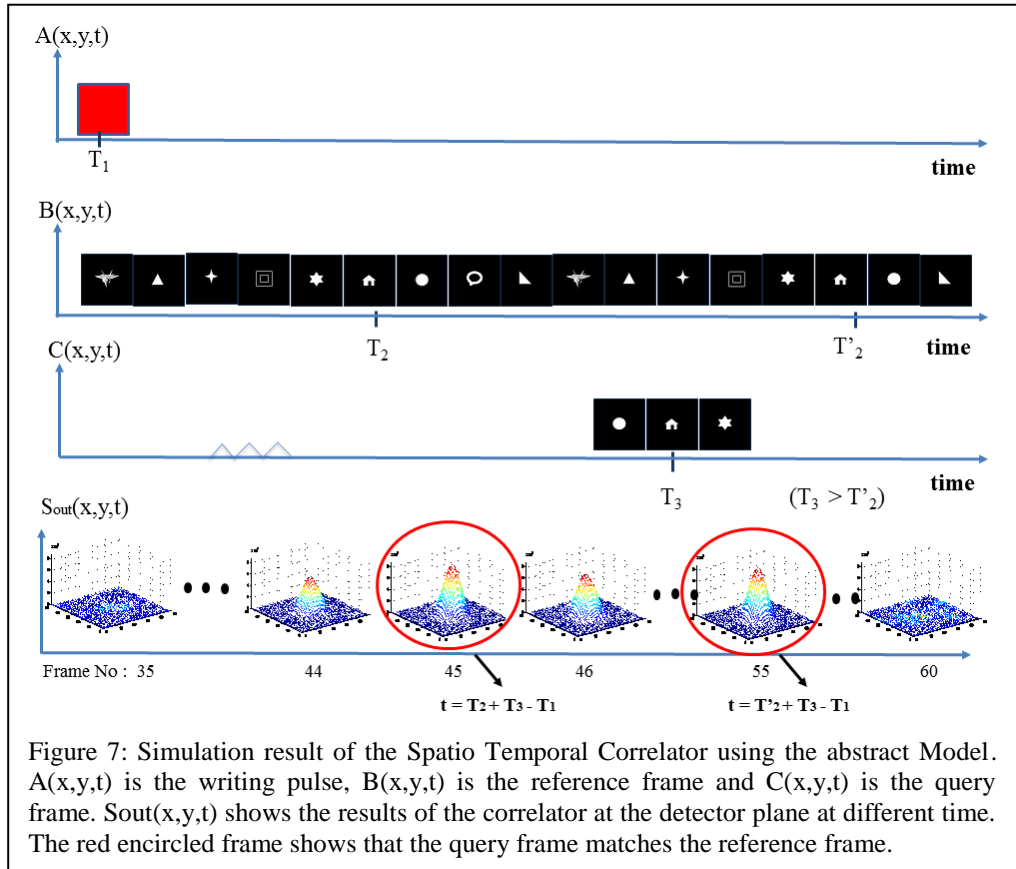


Fig 5: Simulation results of a temporal correlator using (a) the quantum mechanical amplitude equation and (b) the abstract transfer function model. Both model yields the same result with faster simulation time for the abstract model

writing beam, followed by the query data stream, with a certain time lag. After another time lag, when the reference data stream is applied to this memory, a correlation peak is observed in a temporally shift invariant manner. In the simulation shown here, we have used an idealized, decay-free two level system of atoms with an inhomogeneous broadening that is larger than the inverse of the temporal resolution of the data stream, given by the rate at which the frames are retrieved from the SLM. Fig 5(a) is simulated using the quantum mechanical amplitude equations described in Appendix A. This simulation of the atomic model has been performed in a super computer for faster calculation. However, in fig 5(b) we have shown that the use of the transfer function of eqn. 9 yields essentially the same result with faster simulation time than the explicit atomic model.

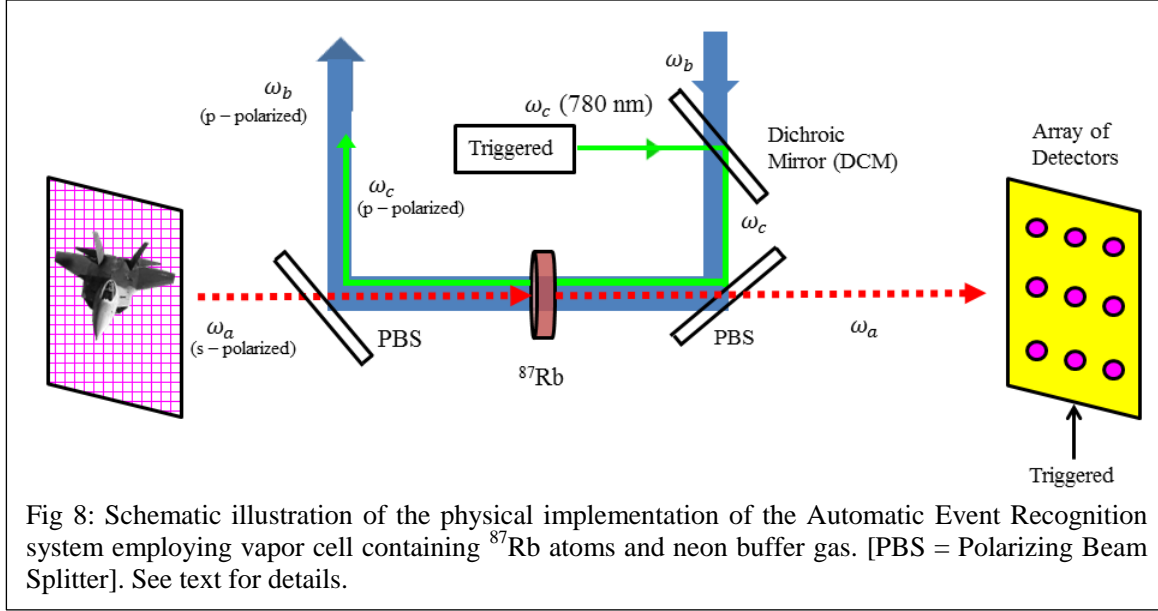
Figure 6 shows the case where we simulate the STC response of an image instead of a single pixel, using the atomic model described in Appendix A as well as using the Abstract model defined by eqns. 9 & 10. For simplicity, a single image is used as the query and reference frame instead of using multiple frames. From the position of the correlation peak in time, we can easily interpret the time where the query image matched the reference image. Here we have also found that the use of the transfer function of eqn. 9 yields essentially the same result as the explicit atomic model, but at a faster rate.

Figure 7 shows the simulation result of the STC using the abstract model, where we have multiple



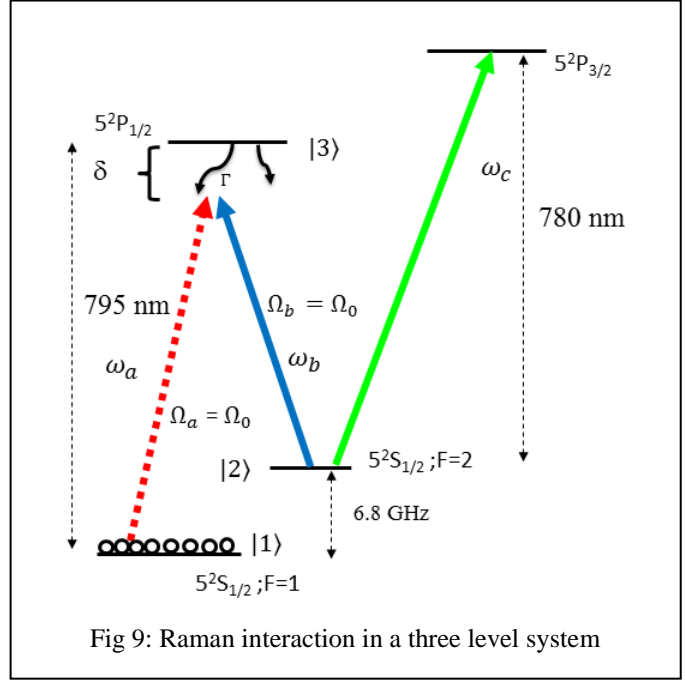
reference and query frames. At time T_1 we apply the write pulse. After that a reference video clip of 20 frames, denoted as $B(x,y,t)$, is applied, $C(x,y,t)$ is the query clip which contains only three frames. Now, using eqns. 9 and 10, we get the signal $S(x,y,t)$, which has highest peak at positions $t = T_3 + T_2 - T_1$ and $t' = T_3 + T'_2 - T_1$.

7. Practical Considerations



The physical implementation of the AER architecture shown in figure 4 is illustrated schematically in figure 8, using ^{87}Rb atoms in a vapor cell as the active medium (without the lenses, for simplicity). The basic process employs an atomic ensemble of three-level Λ - system as shown in figure 9, consisting of levels $|1\rangle$ ($5^2S_{1/2}; F=1$), $|2\rangle$ ($5^2S_{1/2}; F=2$), and $|3\rangle$ ($5^2P_{1/2}$ manifold). The atomic medium, which is assumed to be a vapor cell, at or above the room temperature, is inhomogeneously broadened due to Doppler shifts. A pulsed auxiliary beam (at frequency ω_c) that couples level $|2\rangle$ to the $5^2P_{3/2}$ manifold is used to optically pump the atoms into level $|1\rangle$ before any correlation process starts. To ensure sufficient spectral broadening of the atomic media the two Raman transition laser beams at frequencies ω_a and ω_b are made to be counter-propagating. The beams (at frequency ω_a) that carry the image information as well as the recording pulse are applied along the 1-3 transition, detuned by an amount, δ . The beam (at frequency ω_b) that excites the 2-3 transition is applied at all times, is also detuned by the same

amount, δ . The value of δ is chosen to be much larger than the decay time of level $|3\rangle$, in order to ensure that the three-level system function effectively as a two level system coupling state $|1\rangle$ to state $|2\rangle$ (see appendix B for details). The two Raman transition beams are polarized to be linear and orthogonal to each other. The optical pumping beam at frequency ω_c has the same linear polarization as that of the Raman beam at frequency ω_b . A dichroic mirror is used to combine these two frequencies, made possible by the fact that they differ in wavelengths by ~ 15 nm. The correlation signal appears at frequency ω_a , and passes through the second Polarizing Beam Splitter (PBS). In the detector plane, the correlation signal is detected by the triggered detector array. The resulting voltage signals from all the detectors are integrated to produce the net signal of the AER system.



It should be noted that the durations of the query clip as well as the database video are determined by the speed of the SLM used for loading these frames into the atomic medium. To illustrate this, consider a situation where the query clip has a nominal duration (T_{NOM}) of 20 seconds, if played on a regular monitor. For a video frame rate (F_{VFR}) of 30 per second, this would contain 600 frames. If the SLM has an operating speed of 0.5 ms (defined as T_{SLM}) per frame, then this clip can be loaded into the atomic medium in 300 ms, which is much shorter than the nominal duration (20 seconds) of the query clip. Thus, in the context of the AER, the retrieval duration of a video clip is given by $T_{\text{RET}} = F_{\text{VFR}} * T_{\text{NOM}} * T_{\text{SLM}}$.

A key feature of the atomic medium is that it stores the spatial and temporal interference between the recording pulse and the query frames in the electro-nuclear spin coherence in the form of a coherent superposition between states $|1\rangle$ to $|2\rangle$. As discussed later in this section, the lifetime of this coherence time can be ~ 1 second in a paraffin coated Rb vapor cell. The spatio-temporal correlation process must be carried out within this time window. However, this does not constrain the size of the database video we can search through. Consider a situation where

the memory time (i.e. the coherence time) is T_3 , the time span of the query clip (expressed as its retrieval duration) is T_1 , and the time span for the database video (expressed as its retrieval duration) is T_2 . The correlator is operated for the duration T_3 , during which a fraction (given by T_3/T_2) of the database has been searched. At this point, the AER system is reinitialized by using the optical pumping beam at frequency ω_c (see figure 8), and the same query clip is loaded again. The database is now loaded with a start time of $(T_3 - T_1)$, the AER is operated for another duration of T_3 , and the process is repeated again, with a start time of $2T_3 - T_1$, and so on, until the whole data base has been searched. This sequencing is illustrated schematically in figure 10. The offset of T_1 in the start time of the database is to ensure that the AER would be able to detect the presence of the query clip even if it occurs in-between each segment searched within each memory window.

As noted above, an important parameter for the AER is the lifetime of the electro-nuclear spin coherence. For ^{87}Rb , this lifetime is ~ 1 sec, achieved by coating the walls of the Rb vapor cell with paraffin [20]. As noted above, this memory time is long enough to search matches for query clips with nominal durations of as long as 1 min, for which $T_{\text{RET}} = 900$ ms if $T_{\text{SLM}} = 0.5$ ms, which is typical for an SLM based on liquid crystals. As noted above, the size of the database that can be searched for a match for such a clip is not constrained by these parameters. Much shorter loading time (few microseconds) can be achieved by using an SLM based on quantum wells [21], thus making it possible to apply the AER system for video clips with a much longer nominal duration. The smallest loading time that can be accommodated by the atomic memory is determined by the effective inhomogeneous width of the two-photon transition coupling level $|1\rangle$ to level $|2\rangle$. When the two beams that cause

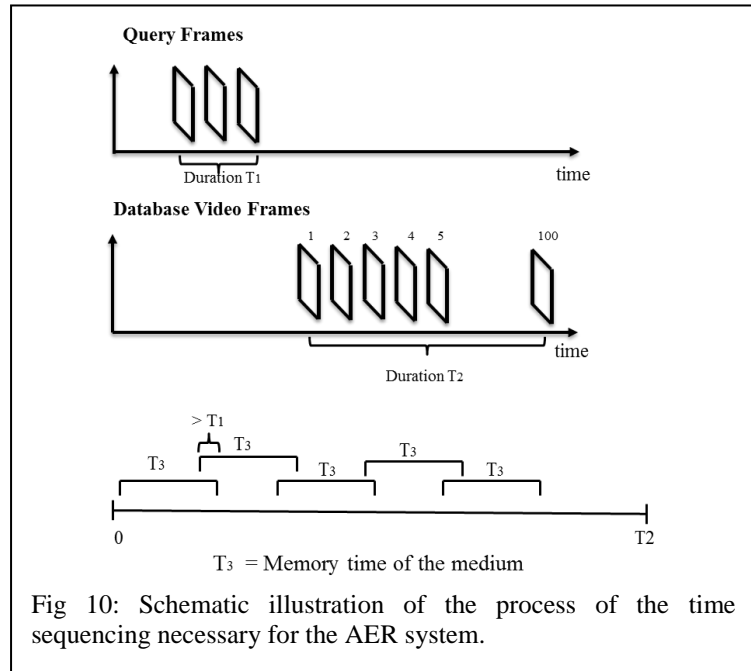


Fig 10: Schematic illustration of the process of the time sequencing necessary for the AER system.

this transition (at ω_a and ω_b) are co-propagating, this width is ~ 11 kHz, which is broad enough

for a loading time of the order of a ms. On the other hand, if the two beams are made to counter-propagate, as shown in figure 9, the inhomogeneous width becomes ~ 1.2 GHz, and this can accommodate SLM loading time as fast as 1 ns.

8. Conclusion

In this paper, we model and simulate a three-dimensional spatio-temporal correlator (STC) that combines the technique of holographic correlation and the technique of photon echo based temporal pattern recognition. The STC is shift invariant in space and time. It can be used to recognize rapidly an event (e.g., a short video clip) that may be present in a large video file, and determine the temporal location of the event. It can also determine multiple matches automatically if the event occurs more than once. The approach we describe makes use of an inhomogeneously broadened Raman transition in an atomic vapor cell.

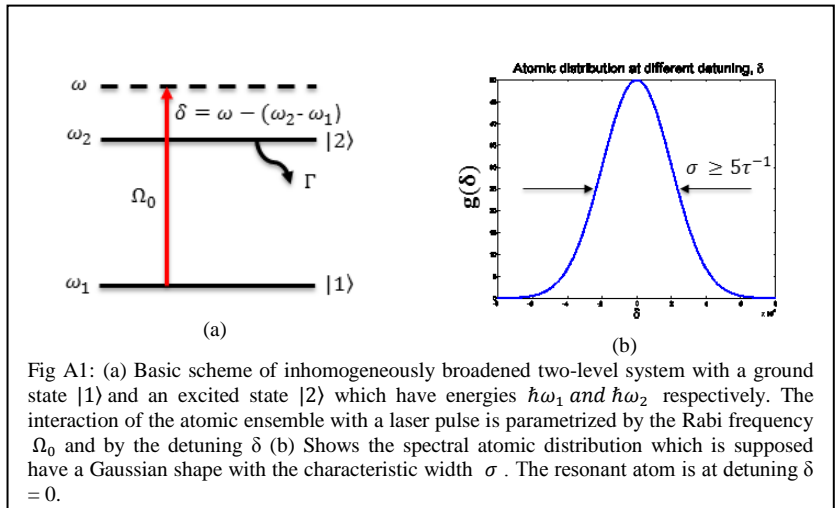
9. Acknowledgements

This work is supported by AFOSR Grant FA9550-10-01-0228.

Appendices

A. Modelling of Two level Atom

Consider a two level system of atomic ensemble excited by a monochromatic field of frequency ω , as illustrated in fig A1(a). Here, $\hbar\omega_1$ and $\hbar\omega_2$ are the energies of levels $|1\rangle$ and $|2\rangle$ which are coupled by a laser field with a Rabi frequency of Ω_0 and a



detuning of δ . The Hamiltonian under electric dipole and rotating wave approximations is given by:

$$H = \hbar \begin{bmatrix} \omega_1 & \frac{\Omega_0}{2} e^{i(\omega t - k z_0 + \phi)} \\ \frac{\Omega_0}{2} e^{-i(\omega t - k z_0 + \phi)} & \omega_2 \end{bmatrix} \quad (1)$$

where k is the wave number of the laser, z_0 is the position of the atom, and ϕ is the phase of the applied electric field. Without loss of generality, we set $z_0 = 0$ and $\phi = 0$ in what follows. The corresponding two level state vector for each atom is

$$|\Psi\rangle = \begin{bmatrix} c_1(t) \\ c_2(t) \end{bmatrix} \quad (2)$$

which obeys the Schrodinger equation: $i\hbar \frac{\partial |\Psi\rangle}{\partial t} = H|\Psi\rangle$. To simplify the calculation, we convert the equations to the rotating wave frame by carrying out the following transformation:

$$|\tilde{\Psi}\rangle = \begin{bmatrix} \tilde{c}_1(t) \\ \tilde{c}_2(t) \end{bmatrix} = Q |\Psi\rangle \quad (3a)$$

$$\text{where, } Q = \begin{bmatrix} e^{i\theta_1 t} & 0 \\ 0 & e^{i\theta_2 t} \end{bmatrix} \quad \text{and} \quad \tilde{H} = Q H Q^{-1} \quad (3b)$$

By choosing $\theta_2 - \theta_1 = \omega$ to eliminate the time dependence, and arbitrarily choosing $\theta_1 = \omega_1$ and $\theta_1 = \omega_1 + \omega$, the Schrodinger equation now can be written as:

$$i\hbar \frac{\partial |\tilde{\Psi}\rangle}{\partial t} = \tilde{H} |\tilde{\Psi}\rangle \quad (4a)$$

$$\text{where, } \tilde{H} = \hbar \begin{bmatrix} 0 & \frac{\Omega_0}{2} \\ \frac{\Omega_0}{2} & -\delta \end{bmatrix} \quad (4b)$$

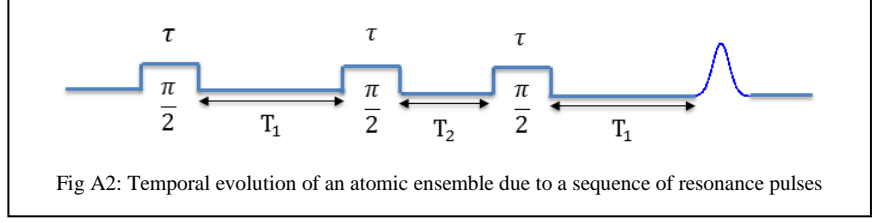
$$\delta = \omega - (\omega_2 - \omega_1) \quad (4c)$$

If we want to include the effect of decay due to spontaneous emission at the rate of Γ from state $|2\rangle$, we must make use of the density matrix equation of motion [19, 22]. However, the practical system we propose to use, as described in appendix B, is an effective two level system involving two metastable states. As such, we can set $\Gamma = 0$ in this model. This allows to us to make use of the amplitude equations (eqn. 4a) to find the temporal evolution of each atom. The general solution of this equation can be expressed as follows:

$$\begin{bmatrix} \tilde{c}_1(t + \Delta t) \\ \tilde{c}_2(t + \Delta t) \end{bmatrix} = e^{i\delta t/2} \begin{bmatrix} \cos\left(\frac{\Omega'\Delta t}{2}\right) - i\frac{\delta}{\Omega'} \sin\left(\frac{\Omega'\Delta t}{2}\right) & -i\frac{\Omega_0}{\Omega'} \sin\left(\frac{\Omega'\Delta t}{2}\right) \\ -i\frac{\Omega_0}{\Omega'} \sin\left(\frac{\Omega'\Delta t}{2}\right) & \cos\left(\frac{\Omega'\Delta t}{2}\right) + i\frac{\delta}{\Omega'} \sin\left(\frac{\Omega'\Delta t}{2}\right) \end{bmatrix} \begin{bmatrix} \tilde{c}_1(t) \\ \tilde{c}_2(t) \end{bmatrix} \quad (5)$$

where, $\Omega' = \sqrt{\Omega_0^2 + \delta^2}$.

To simulate the process of photo echo, we start with an ensemble of two-level systems with a ground state $|1\rangle$ and an



excited state $|2\rangle$ as depicted in figure A1(a). Figure A1(b) shows the spectral atomic distribution which has a Gaussian profile with a width of σ . Due to Doppler shift, the effective detuning seen by an atom moving with a velocity v in the direction of the laser beam is given by $\delta = \delta_o - kv$, where $\delta_o = \omega - \omega_o$ is the detuning of the laser for a stationary atom, $\omega_o = \omega_2 - \omega_1$ is the resonance frequency of the atom. Note that, alternatively, this equivalent to a laboratory frame picture in which the laser frequency is fixed at ω , and an atom with velocity v has a resonance frequency of $\omega_v = \omega_o + kv = (\omega_2 - \omega_1) + kv$, and the detuning experienced by this atom is $\delta = \omega - \omega_v = \omega - (\omega_o + kv) = \delta_o - kv$. For our simulations, we assume the laser to be resonant with the stationary atoms, so that $\omega = \omega_o$, and $\delta_o = 0$. The width σ of the spectral distribution is determined by the thermal velocity spread, and is about 550 MHz for the D_1 transition in ^{87}Rb atoms at a temperature of 100 °C.

We suppose that, initially, all N atoms are prepared in the state $|1\rangle$. We first determine the quantum state of a band of atom, with velocity v , after it has interacted with several laser pulses in sequence. This state is then used to determine the amplitude and phase of the induced dipole moment [proportional to $\rho_{12} \equiv c_1(t)c_2^*(t) = \tilde{c}_1(t)\tilde{c}_2^*(t) e^{i[\delta t + (\omega_2 - \omega_1)t]}$] oscillating at the frequency of $\omega_v = \omega_o + kv$. We then calculate the response of all the atoms with different velocities and add them together, weighted by

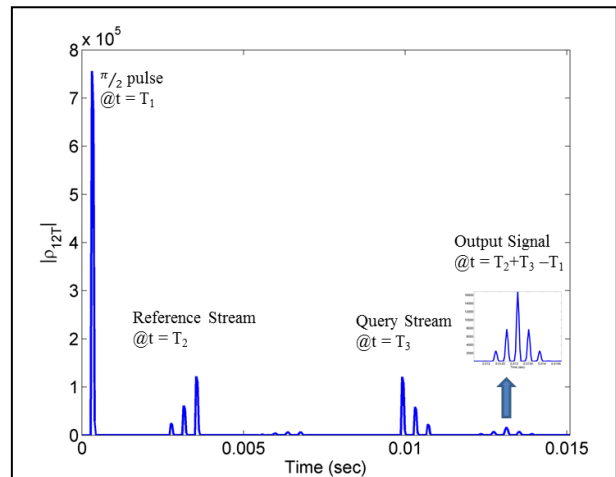


Fig A3: Shows the simulation results of the temporal correlator where the query stream matches the reference stream. The photon echo signal appears at $t = T_2 + T_3 - T_1$

the Gaussian distribution as a function of velocity, to find the net dipole moment. The electric field of the resulting optical pulse is proportional to this net dipole moment. To ensure high-fidelity recording of the pulses in the atomic medium, we ensure that the duration of the shortest light pulse is at least five times longer than the inverse of σ , the width of the atomic spectral distribution.

The process of stimulated photon echo is illustrated schematically in Fig. A2. Here, the atoms are initially prepared in the ground state, so that we have $\tilde{c}_1(t_0 = 0) = 1$ and $\tilde{c}_2(t_0 = 0) = 0$. Here, the first $\pi/2$ pulse is followed, after time T_1 , by two other $\pi/2$ pulses that are separated by a duration of T_2 . The echo appears a duration T_1 after the third pulse. Here, we have assumed that the duration of each pulse is negligible compared to the intervals between the pulses. More generally, if we use the notation that the three pulses are applied at times t_1 , t_2 and t_3 , respectively, with respect to an arbitrary origin of time, then the echo appears at $t_4 = t_2 + t_3 - t_1$. The net dipole moment induced by the photon echo is given by:

$$P(t_4) = \int_{-\infty}^{\infty} \rho_{12}(t_4, \delta) g(\delta) d\delta \quad (6)$$

where $g(\delta)$ is the Gaussian spectral distribution shown in Fig. A1(b).

Consider now a situation where the second pulse is replaced by a small group of pulses (denoted as the reference pulse stream), and the third pulse is replaced by another small group of pulses (denoted as the query pulse stream). If the two pulse streams match each other, then we will get a strong photon echo. This is the manifestation of the atomic temporal correlation process. Fig A3 shows the simulation results of a such a temporal correlator where the query pulse stream matches the reference pulse stream. Hence we get a photon echo at time $t = T_2 + T_3 - T_1$.

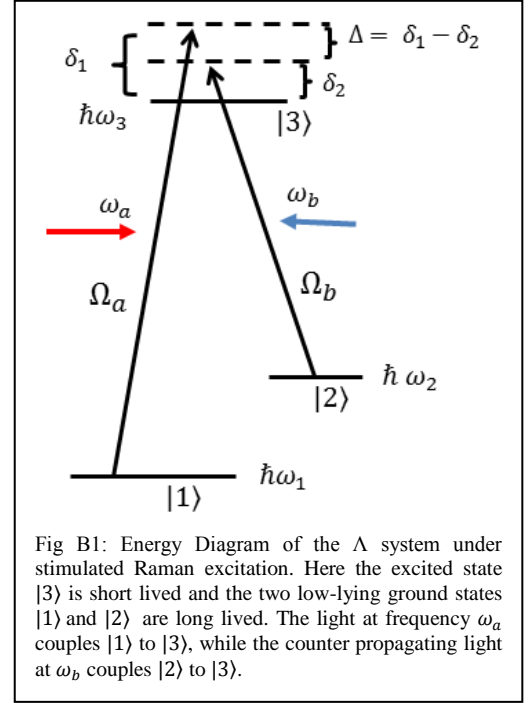


Fig B1: Energy Diagram of the Λ system under stimulated Raman excitation. Here the excited state $|3\rangle$ is short lived and the two low-lying ground states $|1\rangle$ and $|2\rangle$ are long lived. The light at frequency ω_a couples $|1\rangle$ to $|3\rangle$, while the counter propagating light at ω_b couples $|2\rangle$ to $|3\rangle$.

B. Three Level System Representation

Figure B1 illustrates schematically the Λ system under stimulated Raman excitation. Here the excited state $|3\rangle$ is short lived and the two low-lying ground states $|1\rangle$ and $|2\rangle$ are long lived. The light at frequency ω_a couples $|1\rangle$ to $|3\rangle$, while the light at ω_b couples $|2\rangle$ to $|3\rangle$ as shown. Both couplings are electric-dipole interactions, whose strengths are given by the Rabi frequencies

$$\Omega_a = \frac{\mu_{13} \cdot E_1}{\hbar}; \quad \Omega_b = \frac{\mu_{23} \cdot E_2}{\hbar}; \quad (7)$$

where μ is the dipole moment operator matrix element for the corresponding transition. The laser detunings $\delta_1 = \omega_a - (\omega_3 - \omega_1)$ and $\delta_2 = \omega_b - (\omega_3 - \omega_2)$ are used to define the difference detuning as $\Delta = \delta_1 - \delta_2$ and the common mode detuning as $\delta = \frac{1}{2}(\delta_1 + \delta_2)$, where $\hbar \omega_1$, $\hbar \omega_2$ and $\hbar \omega_3$ are the energies of the three levels. Finally, the individual decay rates from state $|3\rangle$ to states $|1\rangle$ and $|2\rangle$ are Γ_{31} and Γ_{32} , respectively, and the total decay rate of state $|3\rangle$ is given by $\Gamma = \Gamma_{31} + \Gamma_{32}$. Here, we assume that $\Gamma_{31} = \Gamma_{32} = \Gamma/2$. In the atomic states basis, the Hamiltonian for the stimulated Raman interaction under the electric dipole and rotating wave approximations is given by:

$$H = \hbar \begin{bmatrix} \omega_1 & 0 & \frac{\Omega_a}{2} e^{i\omega_a t} \\ 0 & \omega_2 & \frac{\Omega_b}{2} e^{i\omega_b t} \\ \frac{\Omega_a}{2} e^{-i\omega_a t} & \frac{\Omega_b}{2} e^{-i\omega_b t} & \omega_3 \end{bmatrix} \quad (8)$$

Similar to what we showed in Appendix A, we can transform the Hamiltonian to the rotating wave basis by using the following matrix [19, 22]:

$$Q = \begin{bmatrix} e^{i\alpha t} & 0 & 0 \\ 0 & e^{i\beta t} & 0 \\ 0 & 0 & e^{i\gamma t} \end{bmatrix}$$

where $\alpha = \omega_1 - \frac{\Delta}{2}$; $\beta = \omega_2 + \frac{\Delta}{2}$. The Hamiltonian can then be expressed as:

$$\tilde{H} = \hbar \begin{bmatrix} \Delta/2 & 0 & \frac{\Omega_a}{2} \\ 0 & -\Delta/2 & \frac{\Omega_b}{2} \\ \frac{\Omega_a}{2} & \frac{\Omega_b}{2} & -\delta \end{bmatrix} \quad (9)$$

If the effect of decay from state $|3\rangle$ is to be taken into account, then we must use the density matrix approach to evaluate the response. However, we limit our system to the condition that $\delta \gg \Gamma, \delta \gg \Omega_0$. Under these conditions, the effect of decay from level 3 can be ignored [19, 22], and using the Hamiltonian of eqn 9, the amplitude equation can be written as:

$$\begin{bmatrix} \tilde{c}_1(t) \\ \tilde{c}_2(t) \\ \tilde{c}_3(t) \end{bmatrix} = -i \begin{bmatrix} \Delta/2 & 0 & \frac{\Omega_a}{2} \\ 0 & -\Delta/2 & \frac{\Omega_b}{2} \\ \frac{\Omega_a}{2} & \frac{\Omega_b}{2} & -\delta \end{bmatrix} \begin{bmatrix} \tilde{c}_1(t) \\ \tilde{c}_2(t) \\ \tilde{c}_3(t) \end{bmatrix} \quad (10)$$

For simplicity consider the case where $\Omega_a = \Omega_b = \Omega_0$. We can make the adiabatic approximation ($\dot{\tilde{C}}_3 \approx 0$) [19, 22], thus yielding the following relations:

$$\begin{aligned} \dot{\tilde{c}}_1(t) &= \left(-i\frac{\Delta}{2} - i\frac{\Omega_0^2}{4\delta} \right) \tilde{c}_1(t) - i\frac{\Omega_0^2}{4\delta} \tilde{c}_2(t) \\ \dot{\tilde{c}}_2(t) &= \left(i\frac{\Delta}{2} - i\frac{\Omega_0^2}{4\delta} \right) \tilde{c}_2(t) - i\frac{\Omega_0^2}{4\delta} \tilde{c}_1(t) \end{aligned}$$

Defining $\epsilon = \frac{\Omega_0^2}{4\delta}$ we can thus write:

$$\tilde{\tilde{H}}' = \hbar \begin{bmatrix} \frac{\Delta}{2} + \epsilon & \epsilon \\ \epsilon & -\frac{\Delta}{2} + \epsilon \end{bmatrix}; \quad |\tilde{\Psi}\rangle = \begin{bmatrix} \tilde{c}_1(t) \\ \tilde{c}_2(t) \end{bmatrix} \quad (11)$$

where the reduce two level system satisfies the Schroedinger equation: $i\hbar \frac{\partial |\tilde{\Psi}'\rangle}{\partial t} = \tilde{\tilde{H}}' |\tilde{\Psi}'\rangle$. Let us further define:

$$|\psi'\rangle \equiv e^{i\theta t} |\tilde{\psi}'\rangle = \begin{bmatrix} C_1' \\ C_2' \end{bmatrix}$$

Using this transformation we can find an effective two level Schrodinger equation of the

form: $i\hbar \frac{\partial |\Psi'\rangle}{\partial t} = H' |\Psi'\rangle$; where $H' = \tilde{\tilde{H}}' - \hbar\theta = \hbar \begin{bmatrix} \frac{\Delta}{2} + \epsilon - \theta & \epsilon \\ \epsilon & -\frac{\Delta}{2} + \epsilon - \theta \end{bmatrix}$; If we choose

$\theta = \frac{\Delta}{2} + \epsilon$, the Hamiltonian can be written as:

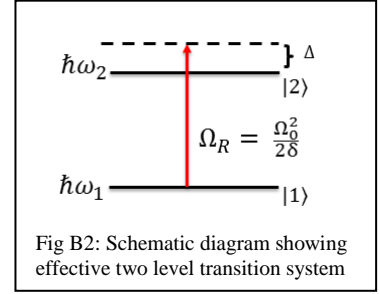
$$H' = \hbar \begin{bmatrix} 0 & \beta/2 \\ \beta/2 & -\Delta \end{bmatrix} \quad (12)$$

where, $\beta = \frac{\Omega_0^2}{2\delta}$; The Hamiltonian of eqn 12 represents an effective two level transition between $|1\rangle$ and $|2\rangle$ with a Rabi frequency β and a detuning Δ as shown in fig B2.

The two level system used in Appendix A now can be viewed as being realized by this reduced system. It should be noted that this effective system involves only the two metastable ground states, and does not include any decay. This justifies the

model we used in Appendix A. Of course, collisional processes cause incoherent exchange of populations between states $|1\rangle$ and $|2\rangle$, and decay of the coherence between these two states. As we have noted in the main body of the paper, the time constant for these processes can be as long as 1 second when paraffin coated vapor cells are used [21]. If the duration of the correlation process is limited to a time much shorter than this time scale, the use of a two level system without any decay or dephasing is justified. It should be noted again that this time scale does not limit the maximum size of the video data base that can be searched, as explained in the main body of the paper.

We also note that for this reduced two level system, the Doppler broadening is manifested in the velocity dependence of Δ . Thus, the effective Doppler broadening is given by the difference (sum) of the Doppler broadening on the two legs of the Raman transition if the lasers are co-propagating, (counter-propagating). Since the inverse of the effective Doppler broadening is a lower limit of the duration of the pulses, it is important to maximize this broadening. Hence, the spatio-temporal correlator we have described in the main body makes use of geometry where the lasers are counter-propagating.



References

1. "Quantum interference and its potential applications in a spectral hole-burning solid," B.S. Ham, P.R. Hemmer, M.K. Kim, and M.S. Shahriar, *Laser Physics* 9 (4): 788-796 (1999)
2. "Demonstration of a phase conjugate resonator using degenerate four-wave mixing via coherent population trapping in rubidium," D. Hsiung, X. Xia, T.T. Grove, P. Hemmer, and M.S. Shahriar, *Opt. Commun.*, 154, 79-82 (1998)
3. "Multidimensional holography by persistent spectral hole burning," A. Renn, U. P. Wild, and A. Rebane, *J. Phys. Chem. A* 106, 3045–3060 (2002)
4. "From spectral holeburning memory to spatial-spectral microwave signal processing," W. R. Babbitt et al., *Laser Physics* 24, 094002 (2014)
5. "Picosecond multiple-pulse experiments involving spatial and frequency gratings: a unifying nonperturbational approach", K. Duppen and D.A. Wiersma, *J. Opt. Soc. Am. B*, 3(4) (April 1986).

-
6. "Translation-Invariant Object Recognition System Using an Optical Correlator and a Super-Parallel Holographic RAM", A. Heifetz, J.T. Shen, J-K Lee, R. Tripathi, and M.S. Shahriar, *Optical Engineering*, 45(2) (2006)
 7. "Shared hardware alternating operation of a super-parallel holographic optical correlator and a super-parallel holographic RAM", M.S. Shahriar, R. Tripathi, M. Huq, and J.T. Shen, *Opt. Eng.* 43 (2) 1856-1861(2004)
 8. "Super-Parallel Holographic Correlator for Ultrafast Database Search," M.S. Shahriar, M. Kleinschmit, R. Tripathi, and J. shen, *Opt. Letts.* 28, 7, pp. 525-527(2003)
 9. "Hybrid Optoelectronic Correlator Architecture for Shift Invariant Target Recognition," Mehjabin S. Monjur, Shih Tseng, Renu Tripathi, John Donoghue, and M.S. Shahriar, *J. Opt. Soc. Am. A*, Vol. 31, Issue 1, pp. 41-47, (January, 2014)
 10. "Shift-Invariant Real-Time Edge-Enhanced VanderLugt Correlator Using Video-Rate Compatible Photorefractive Polymer," A. Heifetz, G.S. Pati, J.T. Shen, J.-K. Lee, M.S. Shahriar, C. Phan, and M. Yamamoto, *Appl. Opt.* 45(24), 6148-6153 (2006)
 11. "All Optical Three Dimensional Spatio-Temporal Correlator for Video Clip Recognition," M. S. Monjur and M.S. Shahriar, in *Proceedings of the Frontiers in Optics and Laser Science Conference*, Tucson, AZ, October, 2014
 12. "Three-dimensional Transfer-function of an Inhomogeneously Broadened Atomic Medium for All Optical Spatio-Temporal Video Clip Correlation," M. S. Monjur and M.S. Shahriar, accepted to appear in *Proceedings of the Frontiers in Optics and Laser Science Conference*, San Jose, CA, October, 2015
 13. "Time Domain Optical Data Storage using Raman Coherent Population Trapping," P.R. Hemmer, M.S. Shahriar, M.K. Kim, K.Z. Cheng and J. Kierstead, *Opt. Lett.* 19, 296 (1994)
 14. "Frequency Selective Time Domain Optical Data Storage by Electromagnetically Induced Transparency in a Rare-earth Doped Solid," B.S. Ham, M.S. Shahriar, M.K. Kim, and P.R. Hemmer, *Opt. Letts.* 22, 1849 (1997)
 15. "From spectral holeburning memory to spatial-spectral microwave signal processing," W. R. Babbitt et al., *Laser Physics* 24, 094002 (2014)
 16. "Optical Header Recognition by Spectroholographic filter," X. A. Shen and R. Kachru, *Opt. Letts.* 20, 2508 (1995)
 17. "Real-time optical waveform convolver cross correlator," Y. S. Bai, W. R. Babbitt, N. W. Carlson, and T. W. Mossberg, *Appl.Phys. Lett.* 45, 714-716 (1984)
 18. "Incorporation of Polar Mellin Transform in a Hybrid Optoelectronic Correlator for Scale and Rotation Invariant Target Recognition," Mehjabin S. Monjur, Shih Tseng, Renu Tripathi, and M.S. Shahriar, *J. Opt. Soc. Am. A*, Vol. 31, No. 6, pp. 1259-1272 (June 2014)
 19. "Evolution of an N-level system via automated vectorization of the Liouville equations and application to optically controlled polarization rotation," *Journal of Modern Optics*, M.S. Shahriar, Ye Wang, S.Krishnamurthy, Y. Tu , G.S. Pati, and S. Tseng, Volume 61, Issue 4, pp. 351-367 (February 2014)
 20. "Nonlinear Magneto-optic Effects with Ultranarrow Widths," D. Budker, V. Yashchuk and M. Zolotarev, *Phys. Rev. Lett.* 81 5788 (1998)
 21. "Enhanced electro-optic effect in GaInAsP/InP three-step quantum wells," H. Mohseni, H. An, Z. A. Shellenbarger, M. H. Kwakernaak, and J. H. Abeles, *Appl. Phys. Lett.* 84, 1823-1826 (2004)

-
22. "Dark-State-Based Three-element Vector Model for the Resonant Raman Interaction," M.S. Shahriar, P. Hemmer, D.P. Katz, A. Lee and M. Prentiss, Phys. Rev. A. 55, 2272 (1997)